

Modeling the Global Structure of the Heliosphere during the Recent Solar Minimum: Model Improvements and Unipolar Streamers

Pete Riley*, Michael Stevens[†], Jon A. Linker*, Roberto Lionello*, Zoran Mikic* and Janet G. Luhmann**

**Predictive Science, San Diego, California.*

[†]*Harvard-Smithsonian Center For Astrophysics, Cambridge, Massachusetts.*

***Space Science Laboratory, University of California at Berkeley, Berkeley, California.*

Abstract. The recent solar minimum, marking the end of solar cycle 23, has been unique in a number of ways. In particular, the polar photospheric flux was substantially weaker, coronal holes were notably smaller, and unipolar streamers were considerably more prevalent than previous minima. To understand the origins of some of these phenomena, we have computed global solutions using a three-dimensional, time-dependent MHD model of the solar corona and heliosphere. In this report, we present a brief overview of a selection of model results, illustrating: (1) how observations are being used to better constrain model properties; and (2) how the model results can be applied to understanding complex coronal and interplanetary phenomena, and, specifically, unipolar streamers.

Keywords: Unipolar streamers, pseudostreamers, coronal holes, MHD modeling, solar cycle

PACS: 96.60.P-, 96.60.pc, 96.60.pf, 96.50.Bh, 96.50.Ci, 96.50.Wx

INTRODUCTION

The recent solar activity minimum, occurring sometime in 2008-2009, depending on its definition, has proved to be unique, at least within the context of solar cycles monitored during the space era, and likely, even on the scale of a century or more [1]. We have studied the interval from the launch of STEREO in October 2006 through the present using a global resistive MHD model of the solar corona and inner heliosphere [2] in an effort to interpret some of the unique features of this interval. In this brief report, we summarize a selection of these investigations. Detailed reports are, or will be presented elsewhere (e.g., [3, 4, 5, 6, 7, 8, 9]). Specifically, we present: (1) two examples where comparisons with remote solar and *in-situ* measurements are providing important feedback for improving the quality of the solutions; and (2) an investigation of the interplanetary signatures of unipolar (also known as pseudo) streamers.

MHD MODELING APPROACH

Our numerical model solves the usual set of resistive MHD equations on a non-uniform grid, in spherical coordinates [10]. Energy transport processes are either included explicitly using the so-called thermodynamic model [11], or conveniently neglected by invoking a polytropic approximation with $\gamma = 1.05$ in the corona and $\gamma = 1.5$ in the

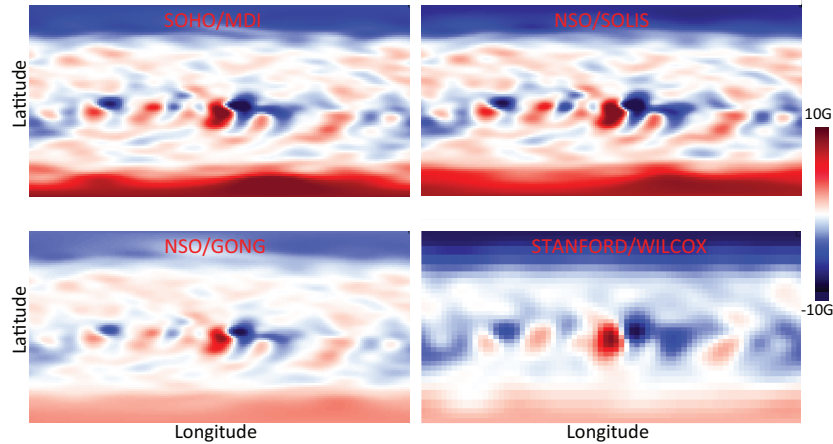


FIGURE 1. Comparison of synoptic magnetograms from four solar observatories for CR 2060. The data have been converted to a radial field, smoothed (by diffusing and filtering the measurements), and, at the highest latitudes, filled, by extrapolating mid-latitude fields poleward.

solar wind [2]. Here we limit ourselves to the polytropic formalism, which allows us to compute solutions more rapidly and hence perform parametric studies of the model inputs.

For the polytropic model, three input variables that can be specified at the lower radial boundary are: (1) the magnetic field vector; (2) the temperature; and (3) the density. Here, we explore the effects of varying the magnetic field and temperature on the resultant solutions. Several processing steps are taken to generate maps that are suitable for the code, which may alter the maps. However, a more fundamental problem exists: We do not have a “ground truth” estimate of the photospheric magnetic field [9]. Figure 1 compares synoptic maps from four solar observatories for Carrington rotation (CR) 2060. While there is a general qualitative agreement, detailed pixel-by-pixel comparisons reveal significant quantitative differences [9]. Additionally, because the Earth’s position is limited in heliographic latitude to $\pm 7.25^\circ$, fields beyond $\sim 65 - 70^\circ$ are poorly resolved, if at all. And finally, synoptic maps are constructed from Earth-based observations: We have no direct observations of the far-side of the Sun and must assume that the Sun does not evolve appreciably over 14-21 days, which is clearly not true. As we will show, these errors propagate through the solution: Speed profiles, for example, computed from different maps show substantial differences, and even the computed total open flux in the heliosphere is significantly affected [12].

A second boundary condition that must be specified in the polytropic model is the temperature at the base, T_o . In reality, thermal processes through the photosphere, chromosphere, and corona will likely produce a complex map of temperatures; however, in our idealization, we assume a constant value for all longitudes and latitudes. Moreover, to maintain a near isothermal corona, consistent with observations, we must reduce γ to a value just slightly above one.

Recently, in a sequence of numerical experiments to investigate the impact of T_o (and the density at the base of the calculation, not considered here), we computed coronal hole boundaries for solutions of CR 2051 for model solutions run with T_o ranging

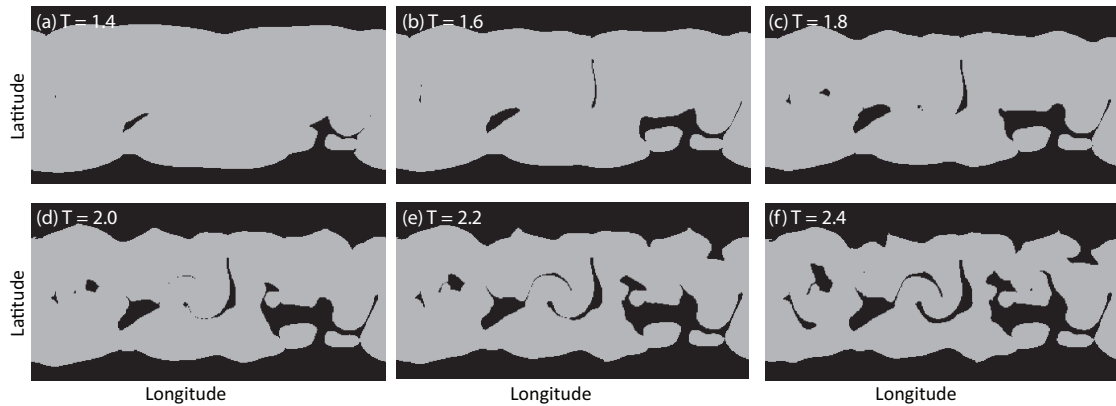


FIGURE 2. Coronal hole boundaries for a sequence of model solutions at different temperatures for CR 2051. The labels give the plasma temperature in units of $\times 10^6\text{K}$. Grey regions represent closed field lines while black indicates field lines that open into the heliosphere.

from $1.4 \times 10^6\text{K}$ to $2.4 \times 10^6\text{K}$ [3]. These are shown in Figure 2. The trends from one panel to the next make intuitive sense. As the base temperature is increased, the thermal pressure also increases as well as the flow speed. More field lines are opened up and the coronal holes grow larger. But which map is correct? Because we are using a polytropic approximation, we cannot constrain T_o directly by observations; it is essentially a free parameter in the model. Instead, we must look to observations that contain structure, such as the coronal hole boundary.

Figure 3 shows SOHO EIT observations at 195 \AA . Coronal holes are readily apparent as dark regions. Superimposed are the computed coronal hole boundaries from four of the model solutions. Based on these comparisons, a temperature, $T_o = 1.8 \times 10^6\text{K}$ seems to match the observations best. Of course there are caveats: EIT observations are a measure of emission, not field-line connectivity. Overlying bright structure, for example, may tend to occlude otherwise dark regions, and EIT observations themselves may underestimate coronal hole size.

The effects of using input synoptic magnetograms from different observatories is explored in Figure 4. From top to bottom, the panels compare solar wind bulk speed at ACE with model solutions driven by data from SOLIS, MDI, GONG, and WSO solar observatories. The implication is clear: different magnetograms can have a profound effect on the quality of the solution [3, 9].

AN APPLICATION OF THE MODEL: UNIPOLAR STREAMERS

Unipolar streamers are structures in the corona that are often indistinguishable in white light observations from the more typical dipolar streamers. However, MHD and potential field source surface models reveal a distinct loop structure within them. Dipolar streamers separate coronal holes of opposite polarity, and so must be composed of a single (or, in principle, triple) loop structure, while unipolar streamers separate holes of the same polarity, and hence contain a double loop structure. Thus, the interplanetary extension of dipolar streamers contains the heliospheric current sheet (HCS), whereas no HCS is

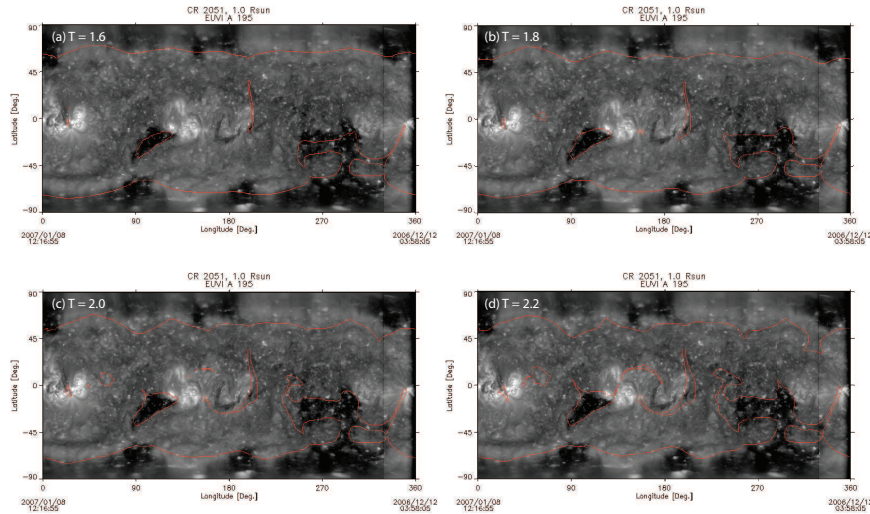


FIGURE 3. SOHO/EIT observations at 195 Å during CR 2051. Panels (a) through (d) differ only in the MHD solution used to produce the computed coronal hole boundaries (red curves).

associated with unipolar streamers.

Models of the slow solar wind predict distinct properties for wind emanating from unipolar streamers. The “expansion factor” model (e.g., [13, 14]), which relies on the super-radial expansion of coronal magnetic flux tubes, predicts a source of very fast wind from unipolar streamers, since the expansion factor associated with these field lines is very low, often close to one. In contrast, models based on the concept of a “boundary layer” between open and closed fields (the interchange reconnection idea (e.g., [15, 16]) being one example) predict slow solar wind from both unipolar and dipolar streamers. We have mapped streamer structure out into the solar wind and *in-situ* measurements back to the Sun in an effort to assess both theories. We found that unipolar sources of solar wind are associated with slow wind [17]. Figure 5 illustrates one of these mapping exercises for CR 2060, during which time there was a clear connection between unipolar structure and measurements at 1 AU in the ecliptic plane.

We also studied earlier time periods analyzed by Neugebauer et al. [18], who wanted to understand the properties and origin of non-HCS interaction regions. Obviously, one might suspect these events to be the interplanetary counterpart of unipolar streamers. They found that non-HCS associated slow solar wind showed properties similar to HCS-associated wind, with the exception that: (1) they were shorter in duration; (2) they had a greater minimum speed; and (3) lower peak and average densities. However, no obvious connection with corona streamers was found. Using our MHD results, we were able to show that unipolar streamers did exist during these intervals. Moreover, the model results were broadly consistent with the observed differences between HCS and non-HCS events.

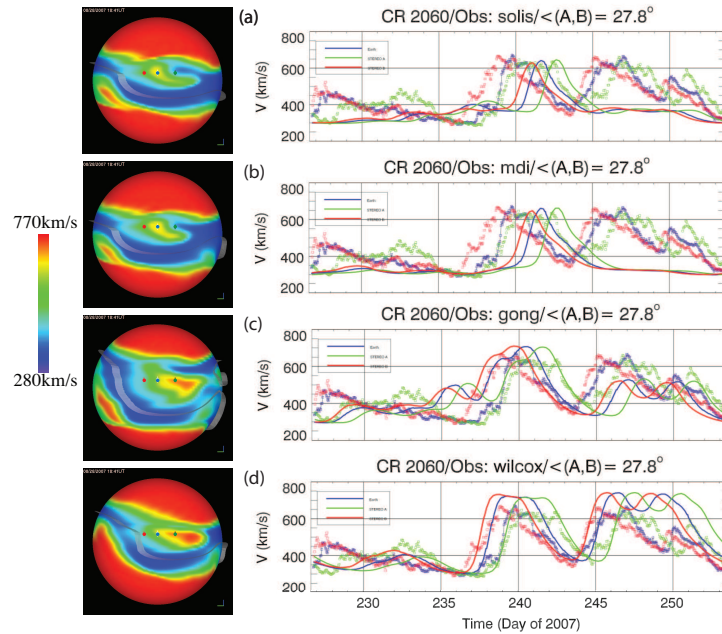


FIGURE 4. (Left) Model solar wind speed at $30R_{\odot}$, together with the location of STEREO A (green), B (red), and ACE (Earth, blue). The HCS is shown by the grey curve. The four panels show results from models driven by data from the following observatories: (a) SOLIS; (b) MDI; (c) GONG; and (d) WSO. (Right) Time series of solar wind speed for the 4 model solutions are compared with data from ACE and STEREO A/B.

SUMMARY AND DISCUSSION

In this report, we have briefly summarized a few studies undertaken to: (1) improve our MHD solutions by comparing with remote solar observations and *in-situ* measurements; and (2) understand some of the unique features of the recent solar minimum. Our analysis has led us to the conclusion that unipolar streamers, when present, can be a significant source of the slow solar wind. Our results also suggest that the “expansion factor” model for the origin of the slow solar wind requires modification to account for slow wind originating from unipolar streamers.

All of the model results presented here are available on the web (www.predsci.com/stereo/). Additionally, NASA’s Community Coordinated Modeling Center (ccmc.gsfc.nasa.gov) provides a web interface for running our model suite (CORHEL) on demand.

ACKNOWLEDGMENTS

We gratefully acknowledge the support of the LWS Strategic Capabilities Program (NASA, NSF, and AFOSR), the NSF Center for Integrated Space Weather Modeling (CISM), NASA’s Heliophysics Theory Program (HTP), the Causes and Consequences of the Minimum of Solar Cycle 24 program, and the STEREO (IMPACT and SECCHI) teams.

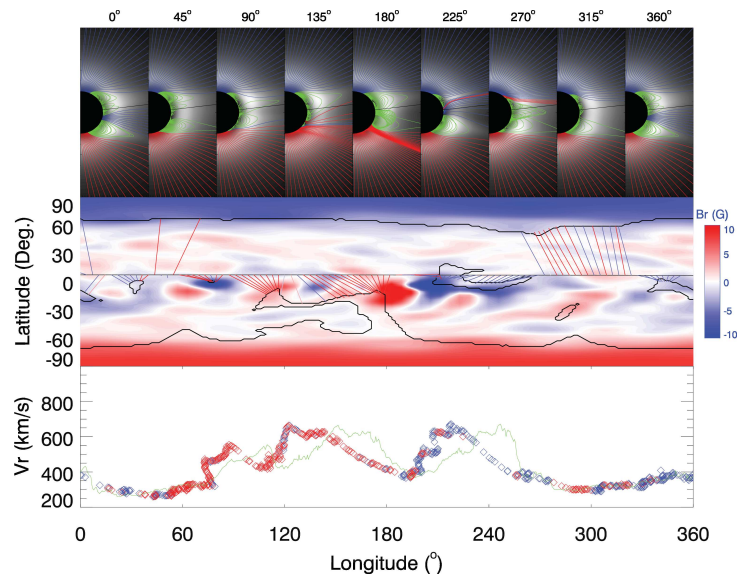


FIGURE 5. (Top) Selection of meridional slices of pB with field lines superimposed. Field lines colored blue (red) open into the heliosphere and are inward (outward). Field lines colored green are closed. The heliographic latitude of ACE is indicated by the solid black line. (Middle) The photospheric magnetic field used to compute the MHD solution. The boundaries of coronal holes are indicated by the black curve and the trajectory of the ACE spacecraft (from right to left as time increases) is shown by the straight black line. Measurements by ACE are mapped back to their inferred source location via the lines branching off the trajectory, color-coded according to the measured *in-situ* polarity. (Bottom) Solar wind speed measured by ACE, mapped back to $30R_{\odot}$, and color-coded with the polarity of the field is shown, together with the mapped plasma density as a function of longitude.

REFERENCES

1. T. Phillips, <http://science.nasa.gov/> (2009).
2. P. Riley, J. A. Linker, and Z. Mikić, *J. Geophys. Res.* **106**, 15889 (2001).
3. M. Stevens, J. A. Linker, and R. P., *Submitted to JASTP* (2011).
4. P. Riley, Z. Mikić, J. A. Linker, J. Harvey, T. Hoeksema, Y. Liu, R. Ulrich, and L. Bertello, *Submitted to Ap. J.* (2010).
5. P. Riley, R. Lionello, J. A. Linker, Z. Mikić, J. Luhmann, and J. Wijaya, *Solar Phys.*, in press (2011).
6. P. Riley, R. Lionello, J. A. Linker, Z. Mikić, J. Luhmann, and J. Wijaya, *Sol. Phys.* pp. 13–+ (2011).
7. P. Riley, and R. Lionello, *Sol. Phys.* pp. 93–+ (2011).
8. P. Riley, J. Luhmann, A. Opitz, J. A. Linker, and Z. Mikić, *J. Geophys. Res. (Space Physics)* **115**, 11104–+ (2010).
9. P. Riley, Z. Mikić, J. A. Linker, J. Harvey, T. Hoeksema, Y. Liu, R. Ulrich, and L. Bertello, *Submitted to Ap. J.* (2011).
10. Z. Mikić, J. A. Linker, D. D. Schnack, R. Lionello, and A. Tarditi, *Phys. Plasmas* **6**, 2217 (1999).
11. R. Lionello, J. A. Linker, and Z. Mikić, *Astrophys. J.* **546**, 542 (2001).
12. P. Riley, *Astrophys. J. Lett.* **667**, L97–L100 (2007).
13. Y. Wang, Y. Ko, and R. Grappin, *Ap. J.* **691**, 760–769 (2009).
14. S. R. Cranmer, *Astrophys. J. Lett.* **710**, 676–688 (2010), 0912.5333.
15. L. A. Fisk, N. A. Schwadron, and T. H. Zurbuchen, *Space Sci. Rev.* **86**, 51–60 (1998).
16. S. K. Antiochos, Z. Mikić, R. Lionello, V. Titov, and J. A. Linker, *submitted to Ap. J.* (2010).
17. P. Riley, and J. Luhmann, *Submitted to Sol. Phys.* (2011).
18. M. Neugebauer, P. C. Liewer, B. E. Goldstein, X. Zhou, and J. T. Steinberg, *J. Geophys. Res.* **109**, 10102–+ (2004).